Materials Today Electronics 11 (2025) 100144

Contents lists available at ScienceDirect

Materials Today Electronics

journal homepage: www.elsevier.com/locate/mtelec

Full Length Article

Design and analysis of junctionless dielectric modulated double-gate GaNFET biosensor for label-free DNA detection

Md. Zahid Hasan [a], Rezaur Raihan [a], Nur Kutubul Alam [a], Md. Rejvi Kaysir [a,b], Md. Shaharuf Islam [c], M. A. Parvez Mahmud [d,*]

[a] Department of Electrical and Electronic Engineering (EEE), Khulna University of Engineering & Technology (KUET), Khulna, 9203, Bangladesh
[b] Photonics Research Group, Department of EEE, KUET, Khulna, 9203, Bangladesh
[c] Environmental Science Discipline, Life Science School, Khulna University, Khulna, 9208, Bangladesh
[d] School of Mathematical and Physical Sciences, University of Technology Sydney, Sydney, NSW 2007, Australia

ARTICLE INFO

Keywords:
DNA detection
Junctionless
GaNFET
Short channel effect
N-type
P-type
Threshold voltage

ABSTRACT

The investigation of DNA hybridization spans various scientific domains, offering insights from genomics to diagnostics and pharmacology. Traditional methods involve labeling DNA, but innovative FET devices use label-free techniques. Nanoscale biosensors provide superior speed, sensitivity, cost-effectiveness, and versatility compared to conventional methods. Overcoming challenges like the Short Channel Effect (SCE) is crucial for synthesizing biosensors meeting these criteria. Previous research focused on junctionless double-gate transistors for mitigating SCE and GaN as channel materials for high-speed, low-power applications. However, dealing with negatively charged biomolecules like DNA poses challenges due to conflicting dielectric constant and interface charge effects. To address these challenges, the proposed nanoscale biosensor employs a junctionless dielectric modulated double-gate GaN field-effect transistor (JL-DM-DG GaNFET). This device effectively synergizes conflicting dielectric constant and charge effects, with GaN as the channel material. Simulation results show the n-type JL-DM-DG GaNFET exhibits significant sensitivity to negatively charged DNA, with a greater change in threshold voltage ($>$ 539 mV for $k = 1$ to $k = 15$) compared to the p-type (-101 mV for $k = 1$ to $k = 4$, and 74.59 mV for $k = 4$ to $k = 15$). Specifically, for charge density the n-type device displays a higher sensitivity 1.05 vs. 0.509 for the p-type and for dielectric constant $k = 16$ (sensitivity 0.8 for n-type vs. 0.4 for p-type). Additionally, the device shows low subthreshold slope ($\sim$ 60 mV/decay) and higher I_{on}/I_{off} ratio, suggesting faster switching and lower power consumption. In summary, the proposed n-type JL-DM-DG GaNFET holds considerable potential for efficient and reliable DNA detection.

1. Introduction

DNA hybridization is crucial for numerous biological and biotechnological processes. In genomics, it compares sequences and identifies mutations [1]. In diagnostics, it detects disease-linked mutations for early diagnosis [2]. In pharmacology, it studies drug-DNA interactions for therapeutic targeting [3]. In gene expression studies, it aids in understanding gene regulation and disease mechanisms [3]. For environmental health, it helps identify pollution and detect pathogens [4]. Polymerase chain reaction (PCR) is the primary method for DNA amplification, crucial for analyzing gene expression levels due to its reliability and efficiency [5]. Alternative DNA detection methods include fluorescence-based techniques, electrochemical assays, enzyme-based strategies, and nanoparticle-based methodologies, each offering unique advantages in sensitivity and specificity [6,7].

Optical measurements, the primary method, require fluorescent materials and costly scanners, limiting portability and complicating in vivo and in situ measurements [8]. While integrating these methods enhances genetic research, techniques like fluorescent, electrochemical, enzymatic, and magnetic involve additional labeling, leading to inefficiencies, complex analysis, and contamination risks [9,10]. Researchers are turning to label-free techniques, which detect DNA hybridization directly by monitoring changes in the recognition layer's properties, simplifying assays, improving accuracy, and reducing artifacts [11].

Field-effect transistor (FET) micro-biosensors, developed through

* Corresponding author at: Senior Lecturer and Program Director, Faculty of Science, University of Technology Sydney, NSW, 2007, Australia.
E-mail addresses: rejvi@eee.kuet.ac.bd (Md.R. Kaysir), Parvez.Mahmud@uts.edu.au (M.A.P. Mahmud).

https://doi.org/10.1016/j.mtelec.2025.100144
Received 24 October 2024; Received in revised form 23 February 2025; Accepted 6 March 2025
Available online 12 March 2025

semiconductor integrated circuit technology, offer miniaturization, standardization, mass production, and integration into smart sensor systems. These sensors detect high-resolution electrical signals from live cells, cell networks, tissues, and organs [12]. Dielectric Modulated Field Effect Transistors (DMFET) have been used for label-free DNA detection, sensing changes in the dielectric constant within a nanogap at the gate dielectric edge [7,13]. In DMFETs, dielectric constant and charge effects influence the threshold voltage (V_T) in opposite directions, reducing sensitivity in n-channel DMFETs. However, p-channel DMFETs enhance sensitivity by synchronizing these effects for negatively charged biomolecules like DNA [7,14].

Then Complementary Metal-Oxide-Semiconductor (CMOS) technology has been employed for biomolecule detection, with significant V_T shifts due to changes in the dielectric constant [13,15]. Advances in nanotechnology have led to label-free biosensors using nanoscale materials, offering superior speed, sensitivity, cost-effectiveness, and versatility [16–18]. However, nanoscale CMOS devices face short-channel effects (SCEs), addressed by junctionless transistors introduced by Colinge et al. [19]. Junctionless transistors are emerging as next-generation devices that effectively address short-channel effects (SCEs) while enhancing overall performance. Among these, Singh [20] focused on dielectric-modulated single-gate Junctionless Field-Effect Transistors (JL-FETs) for biosensing applications, highlighting their potential. However, multi-gate MOSFETs, such as double-gate structures, have also gained attention for their superior sensitivity and performance in biosensing applications . Notably, double-gate MOSFETs (DG-MOSFETs) have demonstrated up to 52 % higher drain current compared to single-gate MOSFETs (SG-MOSFETs), making them more suitable for high-sensitivity biosensing tasks [21–23]. The DG-MOSFET demonstrates 1.2 % higher sensitivity in the transconductance-to-drain current ratio compared to the SG-MOSFET, indicating improved responsiveness to gate voltage variations [21].

Kaur [24] further advanced this area by investigating silicon-based double-gate Junctionless Transistors for biosensing, revealing their enhanced sensitivity.

In recent developments, the researcher used GaN-based materials, with their wide bandgap and high electron mobility, to demonstrate excellent switching characteristics and mitigate SCEs, making them suitable for low-power applications [25–27]. Combining the benefits of 2D materials like GaN with double-gate Junctionless Transistor architectures can be provided a promising pathway for achieving high sensitivity, improved detection, scalability to the nanoscale, and energy-efficient operation, addressing key challenges in modern biosensing and device design.However, synthesizing biosensors that meet all these requirements simultaneously remains challenging. Previous research has focused on junctionless double-gate transistors and explored GaN for high-speed, low-power, and cost-effective solutions. But challenges arise with negatively charged biomolecules like DNA, where dielectric and charge effects counteract, reducing sensitivity [28–30]. This paper proposes a nanoscale biosensor based on a junctionless dielectric-modulated double-gate GaN field-effect transistor (JL-DM-DG GaNFET) to effectively address these issues. The study aims to enhance DNA detection by measuring threshold voltage changes due to dielectric constant and negative charge density alterations in the biosensor's nanogap. The goal is to achieve greater sensitivity and accuracy, minimize short-channel effects, enhance response times, reduce power consumption, and ensure affordability and compactness for chip integration.

2. Materials and methods

2.1. Device structure and simulation method

The device architecture of n-type and p-type JL-DM-DG GaNFET-based nanoscale biosensors used in this work is depicted in Fig. 1. Here, $L_{nanogap}$ is the length of the nanogap cavity; $L_{channel}$ is the channel length.

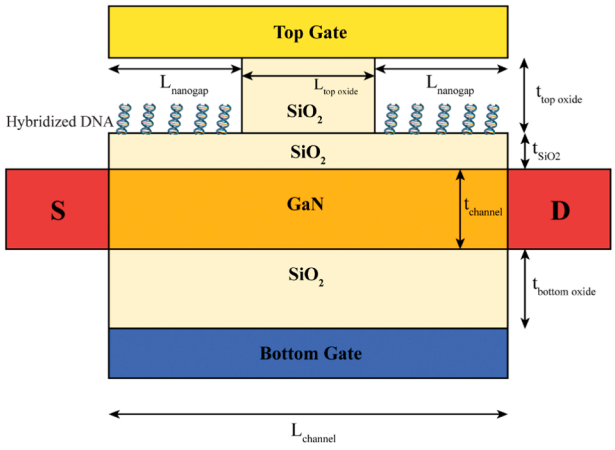

Fig. 1. Schematic diagram of the proposed structure of junctionless dielectric modulated asymmetric double-gate GaN field effect transistor-based nanoscale biosensor.

$t_{topoxide}$, $t_{channel}$, $t_{bottomoxide}$ is the thickness of the nanogap cavity, channel, and gate oxide, respectively. For the device structure, the typical values of different parameters used here are $t_{top\ oxide}$ = 5 nm, $t_{channel}$ = 3.5 nm, $L_{channel}$ = 60 nm, $L_{nanogap}$= 20 nm, and $L_{top\ oxide}$= 20 nm.

A thin SiO_2 layer on the top oxide-channel interface acts as an adhesion layer and is used for the immobilization of biomolecules. Asymmetrical DG MOSFETs with optimized single channels provide higher drive currents at low voltages and enhanced biomolecule recognition sensitivity fivefold due to greater threshold voltage (Vth) shifts, especially for channel lengths ≤50 nm [31,32].Also Sandip Kumar [33] demonstrates significant improvements in DG JLFET performance, achieving an OFF-current of $\sim10^{-14}$ A/μm, an ON-to-OFF current ratio of 10^{10}, and a subthreshold slope of 65.6 mV/dec at a gate work function of 5.1 eV. Comparing work functions from 5.0 eV to 5.3 eV, the threshold voltage (VTH) increases from ~0.257 V to ~0.557 V, while the OFF-current (I_{OFF}) drops from $\sim1.66 \times 10^{-8}$ A/μm to $\sim9.36 \times 10^{-13}$ A/μm. This leads to an exponential ON-to-OFF current ratio improvement from $\sim8.55 \times 10^{4}$ to $\sim8.49 \times 10^{8}$, highlighting the importance of using different materials for the top and bottom gates to optimize electrostatic control and device efficiency . Therefore, gold (work function = 5.3 eV) is used as the top gate material, while cobalt (work function = 5.0 eV) is selected for the bottom gate

For the simulations, magnesium (Mg) is used as the p-type dopant in the source region, while the channel region, composed of wide-bandgap material GaN, is uniformly doped with n-type dopants silicon (Si) to a concentration of $1 \times 10^{19} cm^{-3}$. The same gate voltage applied for both gate. These nanogap cavity regions serve as sensing sites, in which the target biomolecules are immobilized. The recognition layer, consisting of a Self-Assembled Monolayer (SAM) of thiolated DNA probes on a gold surface, is utilized in a practical application [14]. However, its significant influence on biosensor sensitivity—through effects on probe density, stability, orientation, and the device's electrical response via changes in dielectric properties and charge distribution—is not discussed in the context. The oxide layer has a great impact on DNA detection. As we have seen when HfO_2 is used, It does not show any noticeable change in threshold voltage change by changing the nanogap dielectric constant(K) values. GaN is a layered semiconductor with a bulk indirect bandgap of ~3.4 eV. Recent studies have shown intrinsic hole mobility in bulk GaN FETs of up to 1500 cm^2/V-s [34].

The proposed device was modeled using the Silvaco Atlas platform, a Finite Element Method (FEM) solver commonly used to characterize semiconductor devices.To implement this, the process begins with defining the mesh and structure according to the device parameters. Subsequently, the appropriate method(Newton trap) and physics are

specified to solve the problem.Similar studies in the literature show consistent results between simulation (using Silvaco Atlas) and practical implementation [7,35]. In this simulation, the device operates based on the principle of threshold voltage, according to Eqs. (8) and (10).

As Colinge noted, channel lengths as small as 30 nm can be implemented without significant SCE [36]. Mohanty demonstrates that a larger nanogap area can accommodate more bio-targets, thereby amplifying the impact of analytes on the device's performance [22]. Shradhya Singh observed that threshold voltage variation is more pronounced at 50 nm compared to 100 nm and 200 nm [32]. Most studies focus on the 40–60 nm range [32,37–39], and the 60 nm channel length in the JL-Dielectric Modulated-DG GaNFET was chosen for its balance of performance and SCE mitigation. While this study does not explore other lengths, the design leverages the double-gate architecture for enhanced electrostatic control, minimizing threshold voltage roll-off and DIBL. GaN's high electron mobility and breakdown voltage enable effective scaling, and the 60 nm length avoids issues like increased gate leakage and SCE seen at smaller scales. This length ensures reliable operation, fabrication feasibility, and optimal subthreshold slope and on/off current ratio for high-speed performance, though further reduction below 60 nm remains feasible without significant SCE challenges. Mohanty shows that if the size of the nanogap area is large, more bio-targets can be accommodated in this area. As a result, the effect of analytes on the device performance enhances.In Dielectric Modulated Field Effect Transistors (DMFETs) for DNA detection, DNA molecules attach to the surface of the cavity region. This region, often a nanogap, has a recognition layer functionalized with molecules or probes that selectively bind to DNA strands [40]. The gate oxide of the device contains these nanogap cavities, acting as detection sites where biomolecules are anchored. Without biomolecules, these cavities are filled with air, causing a difference in the dielectric constant and shifting the threshold voltage from its initial value. When target DNA molecules are present and bound at these sites, the dielectric constant changes, altering the device's gate capacitance and influencing its electrical characteristics, including the threshold voltage.

2.2. Device physics

Applying a positive potential to the gate electrode of a Junctionless Field-Effect Transistor (JLFET) reduces the width of the depletion layer, creating a neutral region within the channel. This mode of operation, termed partial depletion, allows current flow from the source to the drain. The neutral region, heavily doped, facilitates current flow and is squeezed between depletion regions due to the gate. The threshold voltage for JLFETs is defined as the gate voltage at which the neutral region disappears due to the merging of depletion regions. This differs from MOSFETs, where the threshold voltage is defined at the onset of inversion. An analytical model for negative interface charge density, the threshold voltage in JLFETs is formulated based on this definition [41].

From the basics of semiconductor devices and MOSFETs, we know that the applied gate voltage (V_G) changes the voltage drop across the gate oxide (φ_{ox}) and the surface potential (φ_S), i.e.

$$V_G = V_{FB} + \varphi_{ox} + \varphi_s \tag{1}$$

Where, V_{FB} is the flat-band voltage, which accounts for the charges in the gate oxide and the work function difference between the gate electrode and the semiconductor.

For n-type single gate JLFET the Poisson equation is given by

$$\frac{\partial^2 \varphi(x)}{\partial x^2} = -\frac{\rho}{\varepsilon_{Si}} \tag{2}$$

Where, $\varphi(x)$ is the potential distribution, ρ is the charge density in the silicon film, and ε_{Si} is the permittivity of silicon. The charge density in the silicon channel can be simply given as,

$$\rho = qN_D \tag{3}$$

Where q is the electronic charge and N_D is the donor doping concentration. The surface potential at the Si–SiO_2 interface can be expressed as,

$$\varphi_s = -\frac{qN_D x_{dep}^2}{2\varepsilon_{Si}} \tag{4}$$

The voltage drop across the oxide obtained as,

$$\varphi_{ox} = E_{ox} t_{ox} = -\frac{qN_D x_{dep} t_{ox}}{\varepsilon_{ox}} \tag{5}$$

Where, t_{ox} is the gate oxide thickness and ε_{ox} is the permittivity of SiO_2So, the gate voltage is,

$$V_G = V_{FB} - \frac{qN_D x_{dep}^2}{2\varepsilon_{Si}} - \frac{qN_D x_{dep} t_{ox}}{\varepsilon_{ox}} \tag{6}$$

At the threshold voltage, the entire silicon film is depleted, i.e. the depletion region width (x_{dep}) spans the entire silicon film thickness (t_{Si}). Replacing V_G by V_{Th}, where V_{Th} is the threshold voltage and x_{dep} by t_{Si} in Eq. (6), obtain the final analytical expression for threshold voltage in JLFETs as,

$$V_{Th} = V_{FB} - \frac{qN_D x_{dep}^2}{2\varepsilon_{Si}} - \frac{qN_D x_{dep} t_{ox}}{\varepsilon_{ox}} \tag{7}$$

In a Junctionless double gate FET(JLDGFET), since two gates are used to deplete the entire silicon thickness, one gate has to deplete only half of the silicon film, i.e. $t_{Si}/2$. Therefore, replacing x_{dep} in equation (3.9) by $t_{Si}/2$, we obtain the threshold voltage for a JLDGFET as

$$V_{Th} = V_{FB} - \frac{qN_D x_{dep}^2}{8\varepsilon_{Si}} - \frac{qN_D x_{dep} t_{ox}}{\varepsilon_{ox}} \tag{8}$$

This equation is for n-type JL-DM-DG-FET.

For p-type single gate JLFET the threshold voltage equation is,

$$V_{Th} = V_{FB} + \frac{qN_A x_{dep}^2}{2\varepsilon_{Si}} + \frac{qN_A x_{dep} t_{ox}}{\varepsilon_{ox}} \tag{9}$$

For p type JL DG FET,

$$V_{Th} = V_{FB} + \frac{qN_A x_{dep}^2}{8\varepsilon_{Si}} + \frac{qN_A x_{dep} t_{ox}}{\varepsilon_{ox}} \tag{10}$$

From the Eq. (8) we can see for n type device the V_{th} is increased when both the permittivity of oxide layer is increased and the interface charge density is increased. The change is 4 times in double gate compared to the single gate FET and from Eq. (10) for p-ype, it indicates that the V_{th} is decreased when the permittivity is increased but for increased in charge density the V_{th} is decreased, which analytically shows the effective change in threshold voltage will decrease for p-type device.This is because of negative interface charge density like DNA. If the positive charge density increases, the effects would be reversed and exactly opposite.

3. Results and discussion

We systematically examine the impact of biomolecules on various electrical parameters of the JL-DM-DG GaNFET for label-free DNA detection. First, we explore how neutral and charged biomolecules influence the drain current and device performance. Next, we analyze changes in threshold voltage due to these biomolecules, highlighting shifts in device operation. We then assess the biosensor's sensitivity to minute biomolecule concentration changes. The evaluation continues with the subthreshold slope, providing insights into the sensor's switching behavior and efficiency. Finally, we discuss the I_{on}/I_{off} ratio, showcasing the sensor's ability to distinguish between different biomolecule binding states and its overall efficacy in biosensing

applications.

3.1. Impact of neutral and charged biomolecules on drain current

DNA, a negatively charged biomolecule, influences the dielectric constant of its surrounding environment. For neutral biomolecules, the dielectric constant of the cavity changes when the neutralized DNA is attached [14]. Without DNA, the cavity resembles air (K = 1), but DNA attachment increases the dielectric constant (K > 1). To study the charge effect with varying negative interface charge densities, a constant dielectric constant (K = 1) was maintained.

Both n-type and p-type JL-DM-DG GaNFETs were simulated and analyzed. Fig. 2 shows the drain current versus gate voltage for n-type devices with varying dielectric constants (Fig. 2a) and interface charge densities (Fig. 2b), and for p-type devices with the same variations (Fig. 2c and d).

It does not account for operation with different gate voltages applied to the top and bottom gates; instead, the same gate voltage is used for both. The plots reveal distinct shifts in drain current due to the presence or absence of DNA. For n-type devices, changes in dielectric constant and charge density cause rightward shifts in the curves. For p-type devices, varying the dielectric constant induces leftward shifts, while changing charge concentration results in rightward shifts. Fig. 2b and d show that lower charge densities cause negligible changes, but higher charge densities result in substantial changes, due to the high doping concentration (1×10^{19} no./cm^2) in the junctionless transistor's channel region.

The alignment between the Id-Vg characteristics curve of our proposed Junctionless Field-Effect Transistor (JLFET) and those in existing studies [32,39,42,43] is strikingly similar. Specifically, the observed behavior, where the device displays "on" characteristics with a positive gate-to-source voltage for n-type operation, matches the anticipated performance outlined in the literature. The noticeable rightward shift of the curve with an increase in dielectric constant highlights its sensitivity to such variations, validating its potential for practical applications.

3.2. Threshold voltage

DNA is a large negatively charged biomolecule and is a significant target for detection. Infusing the nanogap with this biomolecule increases the dielectric constant, inducing a shift in the threshold voltage (ΔV_{th}) [14]. Thus enabling the electrical detection of biomolecule binding without labeling. Fig. 3 illustrates that the change in threshold voltage ($\Delta V_{th} = V_{th(bio)} - V_{th(air)}$) for n-type devices (Fig. 3a) exhibits an

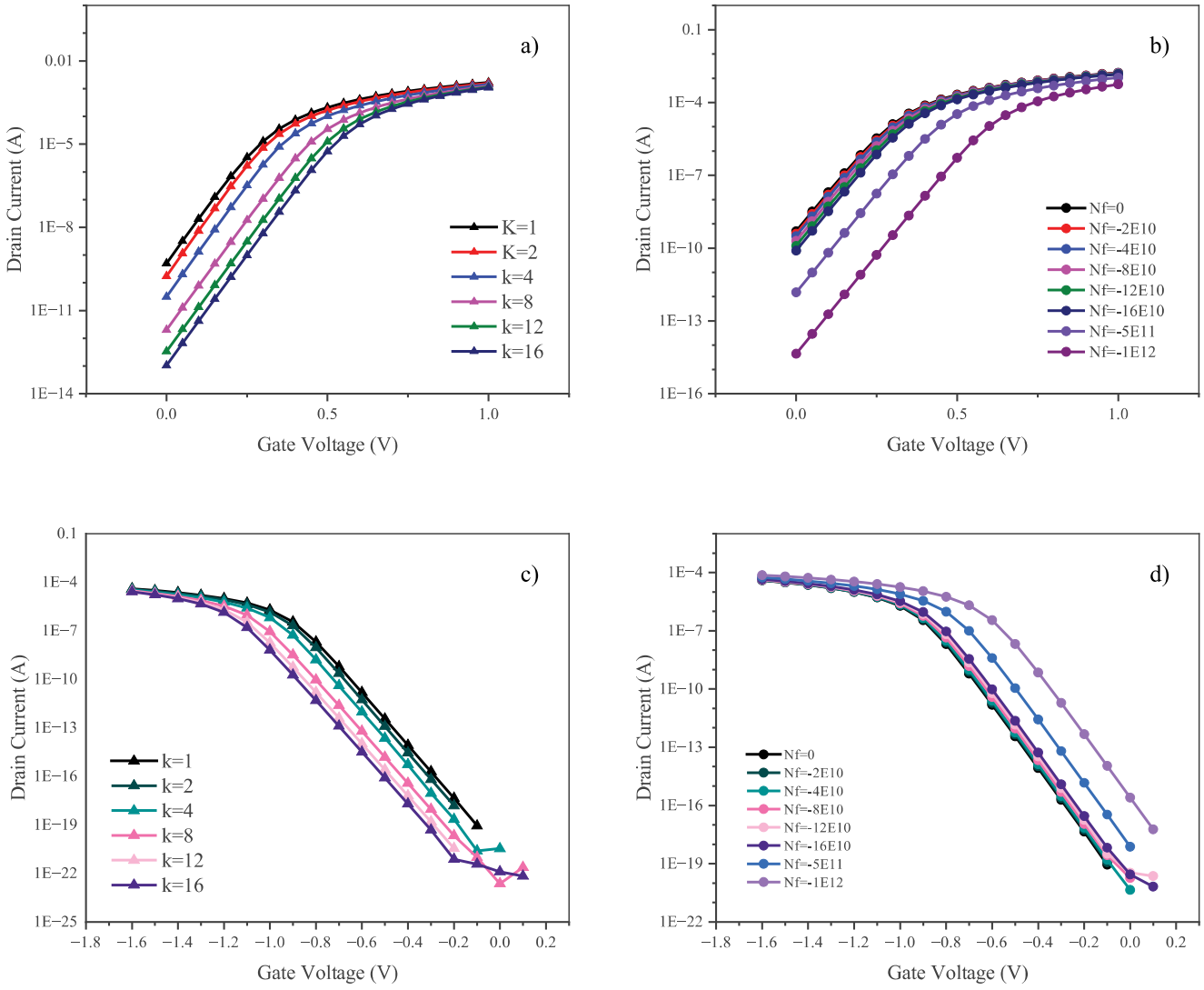

Fig. 2. Variation of drain current with gate voltage for (a) different dielectric constant of neutralized DNA, and (b) different negative charge density when dielectric constant was fixed (K = 1) for *n*-type JL-DM-DG GaNFET. Also, the variation of drain current for (c) different dielectric constant of neutralized DNA and (d) different negative charge density when dielectric constant was fixed (K = 1) for p-type JL-DM-DG GaNFET.

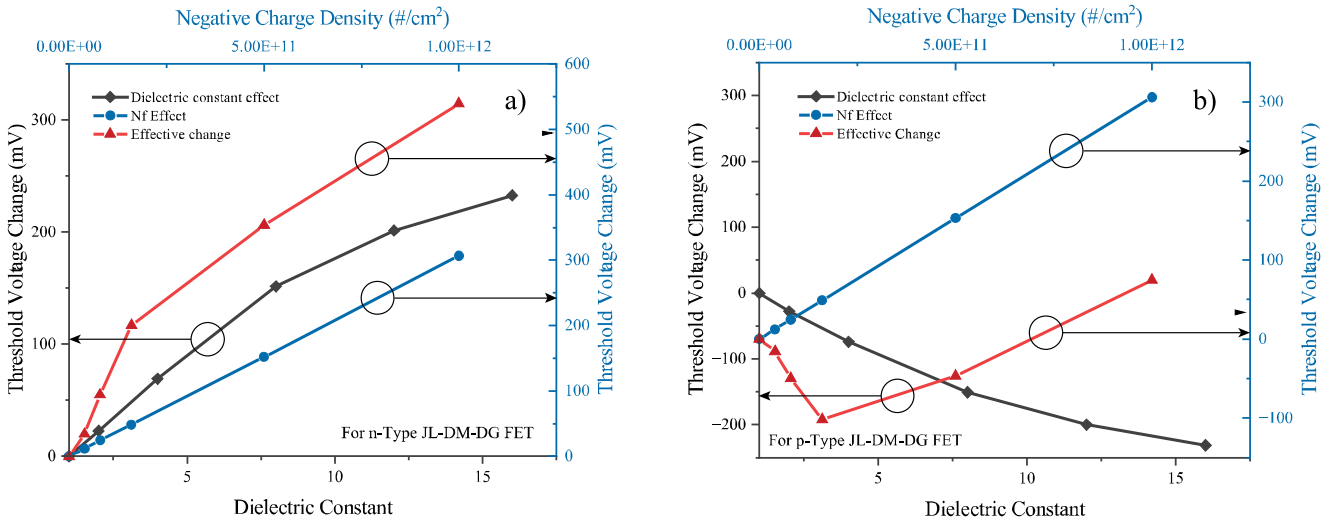

Fig. 3. Variation in threshold voltage change with the increase in the dielectric constant value (bottom *x*-axis) and negative charge density (top *x*-axis) by attaching target DNA in the cavity region of a) n-type JL-DM-DG GaNFET and b) p-type JL-DM-DG GaNFET.

upward trend, indicating an increase in the threshold voltage change in both dielectric constant and negatively charged molecule which is following Eq. (2). As a result, the resultant threshold voltage change is more pronounced in n-type devices. This upward trend suggests a heightened sensitivity, emphasized by the resultant threshold voltage change of 539 mV for $k = 1$ to $k = 15$ which is more pronounced in n-type devices.

Fig. 3(b) shows the variation in threshold voltage for p-type devices, with the curve showing a downward trend indicative of decreasing threshold voltage as the dielectric constant value increases. However, it is noted that the threshold voltage increases when negatively charged DNA is introduced in p-type devices. This behavior is well-matched with Eq. (10). Consequently, the resultant threshold voltage change experiences a reduction of −101 mV for $k = 1$ to $k = 4$, and 74.59 mV for $k = 4$ to $k = 15$.

The interface charge density depends only on the hybridized DNA, as a specific amount of probe DNA is immobilized in the nanogap. Practical studies, including referenced papers, show that the threshold voltage change is due to hybridized DNA alone [14]. Both Fig. 3(a) and (b) illustrate a minimal change in threshold voltage (a few mV) for lower charge densities (0 to 8×10^{10} #/cm^2). Nevertheless, a significant shift in threshold voltage is observed at higher charge densities. DNA detection is influenced not just by interface charge density but also by the dielectric constant effect. As shown in Fig. 3a and b, even at lower interface charge densities, the dielectric constant effect can still produce a detectable signal, confirming the device's sensitivity to both factors. For lower charge density, the dielectric constant dominates, leading to a decrease due to very high (1×10^{19} #/cm^2) channel doping concentration. However, after introducing a sufficient interface charge from attached DNA, the charge effect became dominant, resulting in an increased threshold voltage change. This effective reduction in threshold voltage change diminishes the detection sensitivity in p-type devices when compared to n-type devices. In the case of n-type JL DM DG GaNFET, it has been observed that the device can detect approximately 8×10^{10} DNA molecules per cm^2. This detection capability is influenced by both the dielectric constant effect and charge density simultaneously.However, previous studies [7,14,35] showed that n-type DMFET shows sensitivity to positively charged or neutral biomolecules whereas p-type DMFET shows a great sensitivity for negatively charged biomolecules such as DNA. This is because these studies use traditional junction-based MOSFET. However, a junctionless MOSFET was used in this study. According to Colinge et al. [19], its electrical characteristics are identical to those of conventional MOSFETs, but the physics is quite different. The conduction path is located near the center of the nanowire, and not at the silicon–SiO_2 interfaces. This allows for the electrons to move through the silicon with bulk mobility, which is influenced much less by scattering than the surface mobility experienced by regular transistors. Moreover, the threshold voltage depends on device geometry and doping fluctuation effects in junctionless transistors. Specifically, for n-type junctionless transistors, an elevated dielectric constant results in a higher threshold voltage, requiring a greater gate voltage for current flow. Also, in the case of JL-DM-DG GaNFETs, surface potential plays a crucial role in setting the threshold voltage (V_t) [44].In previous studies, Kaur [24], Chowdhury [45], and Shadman [46] reported effective threshold voltage changes of 3.10 V, 0.023 V, and 0.33 V, respectively, for devices with a dielectric constant of K = 8. In contrast, our proposed n-type JL-DM-DG GaNFET exhibits a more pronounced threshold voltage change of 3.37 V, highlighting its superior performance.

3.3. Sensitivity

The sensitivity of the device can be expressed as

$$Sensitivity = \left| \frac{V_{th(bio)} - V_{th(air)}}{V_{th(air)} \right| \quad (11)$$

Here, Vth(bio) represents the threshold voltage when a biomolecule is attached (K > 1 for neutralized DNA and Nf < 0 for charged DNA), while Vth(air) denotes the threshold voltage in the absence of a biomolecule (K = 1 and Nf = 0 for both neutralized and charged DNA).

Eq. (11) is used to calculate the sensitivity of the device [22,42,45]. Fig. 4 compares the sensitivity of n-type and p-type JL-DM-DG GaNFET devices with respect to dielectric constant (Fig. 4a) and charge density (Fig. 4b). For charge density, the n-type device has a sensitivity of 1.05, exceeding the p-type device's sensitivity of 0.509. This aligns with Eq. (8) and Eq. (10). For a dielectric constant ($k = 16$), the n-type device shows a sensitivity of 0.8, while the p-type device shows 0.4. In both cases, the n-type device demonstrates greater sensitivity.

In n-type JL-DG-FETs, negative charge increases interface charge density, raising V_{th} and enhancing biosensing sensitivity via stronger electrostatic control. In p-type devices, it reduces channel charge, lowering V_{th}, but with a weaker effect due to limited electrostatic modulation.

Comparing these devices with neutral biomolecules, the n-type device shows a steeper curve than the p-type. For negatively charged DNA, the absolute value of sensitivity is significantly higher for the n-type

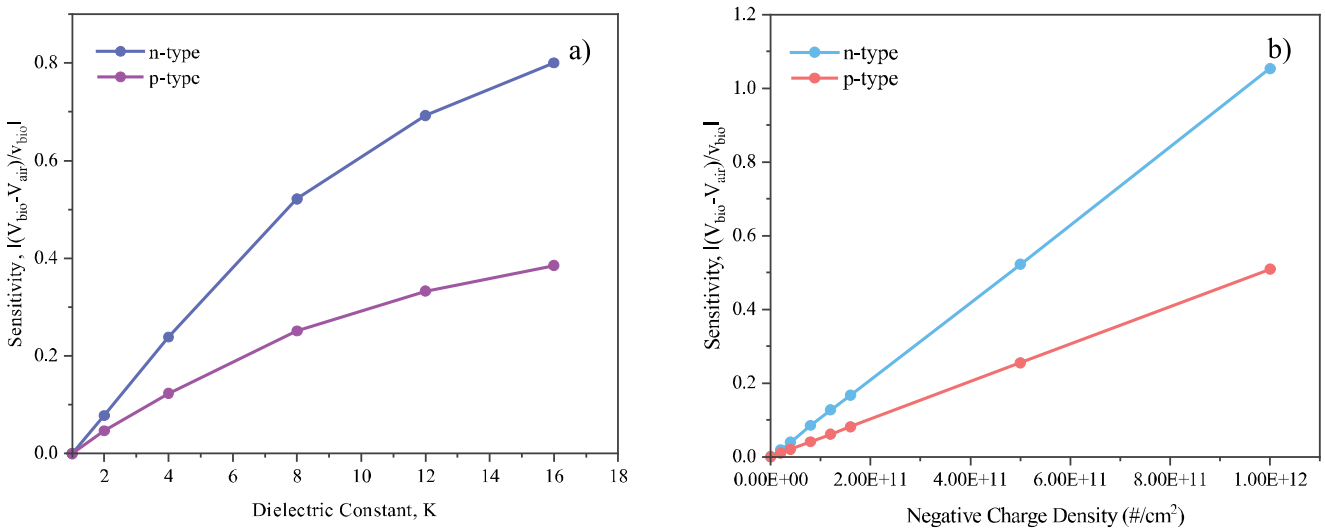

Fig. 4. Variation of sensitivity factor ΔV_{th} for n-type and p-type JL-DM-DG FETs for the increase in a) dielectric constant, and a) negative charge density.

device, indicating a more pronounced behavior change for the same quantity of attached DNA. While previous studies recommended p-type MOSFETs for detecting negatively charged DNA [7,22,35], those devices were not junctionless. Kim [14] reports for DNA, an effective threshold voltage (V_{Th}) shift of 0.4 V for a p-type junction-based FET, whereas for an n-type junction-based FET, the shift is only 0.02 V due to a decrease in its effective voltage. Mohanty [22] shows that their deviceDielectrically Modulated Hetero Channel Double Gate p-type MOSFET has a sensitivity of 0.521 for accumulation of charge -10 × 10^{13} C/m^2 whereas our proposed device shows 0.53 for a very small amount of charge -5 × 10^{11}. Thus, our findings suggest that junctionless n-type devices perform better in detecting negatively charged biomolecules.

3.4. Subthreshold slope

The short-channel effect in MOSFETs typically results in a degraded subthreshold slope, necessitating a higher gate voltage to maintain the same subthreshold current. The proposed junctionless double-gate GaN FET mitigates this effect by eliminating the junction between the source and drain, thereby preventing leakage current caused by carrier diffusion. This design facilitates efficient carrier transport from the source and drain to the channel region, resulting in lower power consumption.. Utilizing GaN as the channel material further enhances device efficiency, sensitivity, and operational speed [47].

As observed, n-type devices exhibit superior performance in DNA detection. Therefore, we focus on further investigating the performance of n-type devices, excluding p-type devices, to enhance low power operation, reduce costs, increase speed, and minimize short-channel effects (SCE). Fig. 5 illustrates the subthreshold slope (SS), a critical parameter in FETs that indicates the rate of change in drain current relative to the gate-to-source voltage in the subthreshold region. The SS is plotted for both dielectric constant, K (Fig. 5a), and negative charge density (Fig. 5b), to evaluate the power consumption and speed of the n-type device. A lower SS is essential for reducing power consumption by improving off-state leakage current control in digital circuits, thereby enhancing energy efficiency. Additionally, a lower SS enables faster switching speeds, crucial for high-speed applications such as RF circuits.

In Fig 5(a), for various K values, the subthreshold slope ranges from approximately 61 to 63 mV/decade, slightly deviating from the theoretical ideal value (for 30 nm) of the subthreshold slope is 60 mV/decade [19]. Similarly, for charge density (Fig. 5b), is <62 mV/decade. Therefore, the consistent and low subthreshold slope across varying dielectric constant and interface charge density indicate effective mitigation of the short-channel effect. The current study focused on

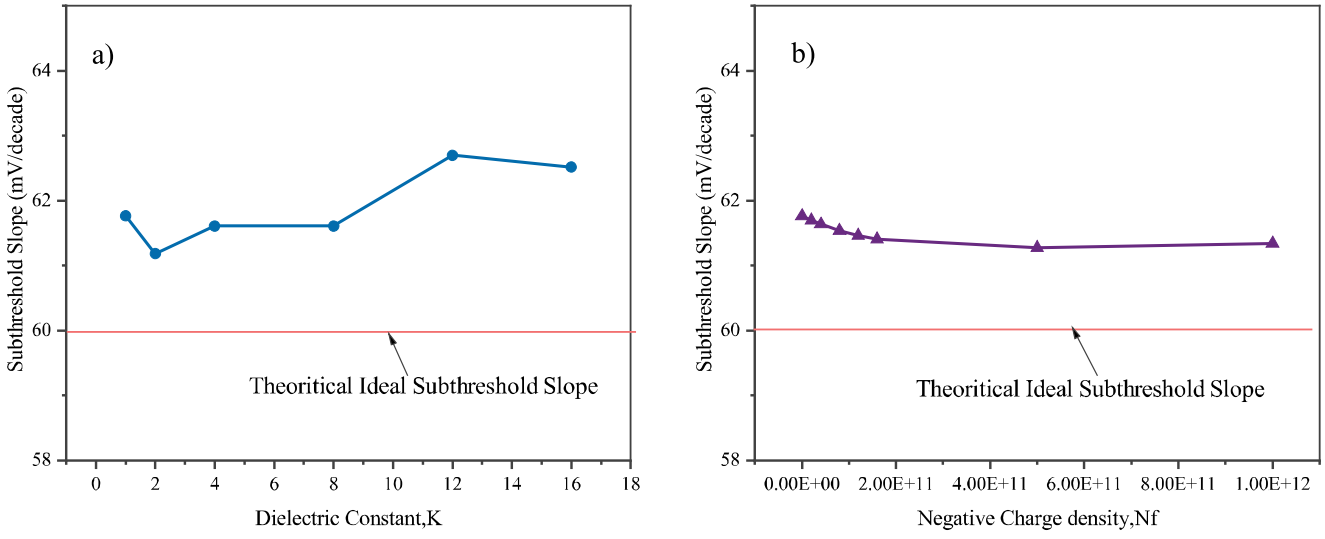

Fig. 5. Variation in subthreshold slope for an n-type device for a) dielectric constant, and b) negative charge density.

demonstrating that at a 60 nm channel length, the device effectively avoids short-channel effects (SCE) and operates smoothly, which is typically unfeasible for conventional MOSFETs. For this reason, It was not explored other channel lengths in this study. However, additional plots of subthreshold slope (SS) against varying channel lengths for different dielectric constants and negative charge densities could provide further validation in future work. This allows the transistor to transition more efficiently between off and on states, reducing power consumption during switching and enhancing the overall speed of electronic circuits. The device demonstrates very fast operation and low power consumption. For example, for $k = 8$ Kaur [24], Kumar [28], Chandan [48], and Wadhwa [39] found the subthreshold slope value to be 63.80 mV/decade, 65.45 mV/decade, 70.32 mV/decade, and 67 mV/decade respectively. Whereas, the proposed device value is 62 mV/decade which indicates the device is faster and low power operation than the above-mentioned devices.

3.5. I_{on}/I_{off} ratio

A higher I_{on}/I_{off} ratio is indicative of enhanced switching efficiency, lower power consumption, and reduced dynamic power dissipation. It reflects the ability of the transistor to effectively switch between the on and off states, representing the contrast between the current levels when the device is conducting and when it is non-conducting. The I_{on}/I_{off} current ratio curve for the dielectric constant effect (Fig. 6a) and charge density effect (Fig. 6b) for the n-type device, exhibits a sharp increase in I_{on}/I_{off} ratio with rising values of dielectric constant (K) and charge density [49]. The I_{on}/I_{off} ratio for both dielectric constant and charge effect for the proposed device is high. The increasing slope is almost exponential after attaching DNA in the cavity.

Here, the I_{on}/I_{off} ratio is 1×10^9 for $k = 8$, 1.1×10^{10} for $k = 16$ (Fig. 6a), and 1.3×10^{11} for N_f=-1×10^{12} #/cm^2 (Fig. 6b) which indicates a very high I_{on}/I_{off} ratio and device performance superiority. This is also evident by the similar studies by Kaur [24], Chandan [48], and Chowdhury [45], where they found the I_{on}/I_{off} ratio to be 2×10^7, 8×10^6 and 2×10^8respectively for $k = 8$. This characteristic is crucial for applications demanding rapid and precise switching, as seen in digital circuits. The lower off-state leakage current (I_{off}) associated with a higher on-off ratio reduces power consumption and maintains a favorable signal-to-noise ratio. So the proposed device demonstrates superior performance compared to the devices discussed in the aforementioned studies. The elevated on-off ratio also results in diminished power dissipation, particularly in applications where dynamic power consumption is a concern, such as in digital circuits.

The performance comparison parameters of the proposed device with the existing literature are summarized in Table 1 where Dielectric constant, K = 8, while the charge density varies. Most of the studies reviewed primarily focus on devices operating under higher charge densities. However, our findings demonstrate superior results even at comparatively lower charge densities. This highlights the efficiency and sensitivity of the proposed device in detecting biomolecules under conditions that require lower input charge densities, offering an advantage in applications demanding minimal charge variations.

4. Conclusion

This study demonstrates the potential of the JL-DM-DG GaNFET for simplifying DNA detection in a label-free, cost-effective, and fast manner. A junctionless dielectric-modulated double-gate GaNFET device was proposed and evaluated for both n-type and p-type configurations. Simulations revealed that the n-type device exhibited a greater threshold voltage change in response to negatively charged DNA compared to the p-type, indicating higher sensitivity. Additionally, the n-type device showed a low subthreshold slope and a high Ion/Ioff ratio, suggesting faster switching speeds and lower power consumption. In conclusion, the proposed n-type JL-DM-DG GaNFET holds significant promise for efficient and reliable DNA detection. We acknowledge that this study does not address the impact of noise and signal variability on the biosensor's performance, which could influence its sensitivity and reliability. Additionally, it does not consider operation under varying gate voltages for both the top and bottom gates. Future research will focus on these aspects to enhance real-world applicability.

CRediT authorship contribution statement

Md. Zahid Hasan: Writing – original draft, Software, Resources, Methodology, Investigation, Formal analysis, Conceptualization. **Rezaur Raihan:** Supervision, Project administration. **Nur Kutubul Alam:** Validation, Software, Methodology, Conceptualization. **Md. Rejvi Kaysir:** Writing – review & editing, Visualization. **Md. Shaharuf Islam:** Writing – review & editing, Visualization. **M. A. Parvez Mahmud:** Writing – review & editing, Visualization.

Declaration of competing interest

The authors declare that they have no known competing financial interests or personal relationships that could have appeared to influence the work reported in this paper.

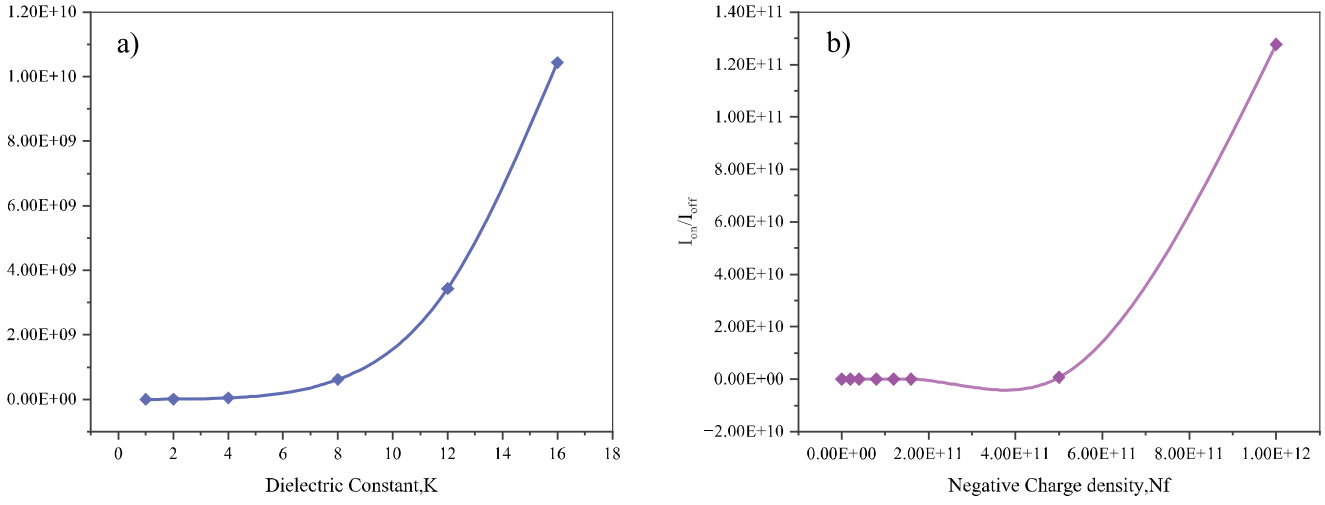

Fig. 6. Variation of Ion/Ioff ratio with a) dielectric constant and b) negative charge density for n-type JL-DM-DG FET.

Table 1
Performance comparison of parameters of the proposed device with contemporary studies.

Device Parameter	Proposed Device	Kaur, et al. [24]	Kumar and Chauhan [28]	Chandan, et al. [48]	Chowdhury, et al. [45]	Shadman, et al. [46]	Mohanty, et al. [22]
Nf(cm^{-2})	-5×10^{11}	-4×10^{12}	–	-3×10^{12}	-4×10^{12}	$\pm 3 \times 10^{16}$	-10×10^{13}
Subthreshold Slope (mV/decade)	62	63.80	65.45	46	70.32		
I_{on}/I_{off}	1×10^9	2×10^7	1×10^{10}	8×10^6	2×10^8		
Threshold Voltage Change (V)	0.37	0.31			0.023	0.33	
Sensitivity	0.53	–			0.48		0.52

Data availability

Data will be made available on request.

References

[1] J.-C. Cho, J.M. Tiedje, Bacterial species determination from DNA-DNA hybridization by using genome fragments and DNA microarrays, Appl. Environ. Microbiol. 67 (8) (2001) 3677–3682.

[2] J. Goris, K.T. Konstantinidis, J.A. Klappenbach, T. Coenye, P. Vandamme, J. M. Tiedje, DNA–DNA hybridization values and their relationship to whole-genome sequence similarities, Int. J. Syst. Evol. Microbiol. 57 (1) (2007) 81–91.

[3] J.P. Meier-Kolthoff, H.-P. Klenk, M. Göker, Taxonomic use of DNA G+ C content and DNA–DNA hybridization in the genomic age, Int. J. Syst. Evol. Microbiol. 64 (Pt_2) (2014) 352–356.

[4] R. Liao, et al., DNA-based engineering system for improving human and environmental health: identification, detection, and treatment, Nano Today 35 (2020) 100958, https://doi.org/10.1016/j.nantod.2020.100958, 2020/12/01/.

[5] W.M. Freeman, D.J. Robertson, K.E. Vrana, Fundamentals of DNA hybridization arrays for gene expression analysis, Bio. Techniq. 29 (5) (2000) 1042–1055.

[6] Z. Ge, H. Pei, L. Wang, S. Song, C. Fan, Electrochemical single nucleotide polymorphisms genotyping on surface immobilized three-dimensional branched DNA nanostructure, Sci. China Chem. 54 (2011) 1273–1276.

[7] C.-H. Kim, C. Jung, K.-B. Lee, H.G. Park, Y.-K. Choi, Label-free DNA detection with a nanogap embedded complementary metal oxide semiconductor, Nanotechnology 22 (13) (2011) 135502, https://doi.org/10.1088/0957-4484/22/13/135502.

[8] O. Yaghmazadeh, et al., In-vivo measurement of radio frequency electric fields in mice brain, Biosensors Bioelectr.: X 14 (2023) 100328, https://doi.org/10.1016/j.biosx.2023.100328, 2023/09/01/.

[9] G. Hanspach, S. Trucks, M. Hengesbach, Strategic labelling approaches for RNA single-molecule spectroscopy, RNA Biol 16 (9) (2019) 1119–1132, https://doi.org/10.1080/15476286.2019.1593093, 2019/09/02.

[10] C.Y. Zhou, S.C. Alexander, N.K. Devaraj, Fluorescent turn-on probes for wash-free mRNA imaging via covalent site-specific enzymatic labeling, Chem. Sci. 8 (10) (2017) 7169–7173, https://doi.org/10.1039/C7SC03150E.

[11] G. Dutta, J. Rainbow, U. Zupancic, S. Papamatthaiou, P. Estrela, D. Moschou, Microfluidic devices for label-free DNA detection, Chemosensors 6 (4) (2018) 43.

[12] L. Ma, et al., Modeling and simulation analysis of junctionless transistors with double gates, J. Phys. Conf. Ser. 2419 (1) (2023) 012082, https://doi.org/10.1088/1742-6596/2419/1/012082, 2023/01/01.

[13] J. Musayev, Y. Adlgüzel, H. Külah, S. Eminoğlu, T. Akln, Label-free DNA detection using a charge sensitive CMOS microarray sensor chip, IEEE Sens J 14 (5) (2014) 1608–1616.

[14] C.-H. Kim, C. Jung, H.G. Park, Y.-K. Choi, Novel dielectric modulated field-effect transistor for label-free DNA detection, Biochip J 2 (2) (2008) 127–134.

[15] S. Kim, J.-H. Ahn, T.J. Park, S.Y. Lee, Y.-K. Choi, Charge pumping technique to analyze the effect of intrinsically retained charges and extrinsically trapped charges in biomolecules by use of a nanogap embedded biotransistor, Appl. Phys. Lett. 96 (5) (2010).

[16] M. Sivaji, M. Yuvaraj, E.T. Hussien, T. Thilagavathi, P. Ayyadurai, Nano-biosensing for detection of food contaminants, in: M.R. Goyal, S.K. Mishra, S. Kumar Eds (Eds.), Nanotechnology Horizons in Food Process Engineering, 1 ed, Apple Academic Press, New York, 2023, p. 28, ch. 2.

[17] S. Chen, et al., Advances in electronic nano-biosensors and new frontiers in bioengineering, in: 2022 International Electron Devices Meeting (IEDM), 2022, pp. 17.1.1–17.1.4, https://doi.org/10.1109/IEDM45625.2022.10019512, 3-7 Dec. 2022.

[18] N. Mandal, A. Das, R.S. Moirangthem, In-situ label-free optical biosensing with plasmonic enhanced ellipsometry using partially-embedded bimetallic Ag-Au alloy nanoparticles, Sens. Actuators B 379 (2023) 133164, https://doi.org/10.1016/j.snb.2022.133164, 2023/03/15/.

[19] J.-P. Colinge, et al., Nanowire transistors without junctions, Nat. Nanotechnol. 5 (3) (2010) 225–229.

[20] D. Singh, G.C. Patil, Dielectric-modulated bulk-planar junctionless field-effect transistor for biosensing applications, IEEE Trans. Electron Devices 68 (7) (2021) 3545–3551.

[21] M.K. Jethwa, H.M. Devre, Y. Agrawal, R. Parekh, A comparative study of MOSFET (Single and Double Gate), silicon nanowire FET, and CNTFET by varying the oxide thickness, in: Proceeding of Fifth International Conference on Microelectronics, Computing and Communication Systems, Singapore, Springer Singapore, 2021, pp. 205–216.

[22] S.S. Mohanty, S. Mishra, M. Mohapatra, G.P. Mishra, Dielectrically modulated hetero channel double gate MOSFET as a label free biosensor, Trans. Elect. Elect. Mater. 23 (2) (2022) 156–163, https://doi.org/10.1007/s42341-021-00334-z.

[23] E.-S. Liu, "Electronic and spintronic transport in germanium nanostructures," 2014.

[24] P. Kaur, A.S. Buttar, B. Raj, Design and performance analysis of proposed biosensor based on double gate junctionless transistor, Silicon 14 (10) (2022) 5577–5584.

[25] I.M. Mehedi, A.M. Alshareef, M.R. Islam, M.T. Hasan, GaN-based double-gate (DG) sub-10-nm MOSFETs: effects of gate work function, J. Comput. Electron. 17 (2018) 663–669.

[26] A. Talukdar, A.K. Raibaruah, K.C.D. Sarma, Dependence of electrical characteristics of Junctionless FET on body material, Procedia Comput. Sci. 171 (2020) 1046–1053.

[27] B. Wang, et al., Ballistic transport in sub-10 nm monolayer planar GaN transistors for high-performance and low-power applications, Appl. Phys. Lett. 119 (16) (2021).

[28] S. Kumar, R.K. Chauhan, A novel dielectric modulated misaligned double-gate junctionless MOSFET as a label-free biosensor, Eng. Proceed. 35 (1) (2023), https://doi.org/10.3390/IECB2023-14578.

[29] A. Biswas, C. Rajan, D.P. Samajdar, A novel HM-HD-RFET biosensor for label-free biomolecule detection, J. Electron. Mater. 51 (11) (2022) 6388–6396, https://doi.org/10.1007/s11664-022-09872-5, 2022/11/01.

[30] S. Yadav, A. Das, S. Rewari, Dielectrically-modulated GANFET biosensor for label-free detection of DNA and Avian influenza virus: proposal and modeling, ECS J. Solid State Sci. Technol. 13 (4) (2024) 047001, https://doi.org/10.1149/2162-8777/ad3364.

[31] K. Kim, J.G. Fossum, Double-gate CMOS: symmetrical-versus asymmetrical-gate devices, IEEE Trans. Electron Devices 48 (2) (2001) 294–299.

[32] S. Singh, S. Bala, B. Raj, B. Raj, Improved sensitivity of dielectric modulated junctionless transistor for nanoscale biosensor design, Sens. Lett. 18 (4) (2020) 328–333, https://doi.org/10.1166/sl.2020.4224.

[33] S. Kumar, A.K. Chatterjee, R. Pandey, Performance analysis of gate electrode work function variations in double-gate junctionless FET, Silicon 13 (10) (2021) 3447–3459, https://doi.org/10.1007/s12633-020-00774-x, 2021/10/01.

[34] N. Hasan, M.R. Islam, and M.T. Hasan, "GaN-based low-power JLDG-MOSFETs: effects of doping and gate work function," 2023.

[35] S. Kalra, M.J. Kumar, A. Dhawan, Dielectric-modulated field effect transistors for DNA detection: impact of DNA orientation, IEEE Elect. Device Lett. 37 (11) (2016) 1485–1488.

[36] J.-P. Colinge, et al., Nanowire transistors without junctions, Nat. Nanotechnol. 5 (2010) 225–229.

[37] E. Rahman, A. Shadman, I. Ahmed, S.U.Z. Khan, Q.D. Khosru, A physically based compact I–V model for monolayer TMDC channel MOSFET and DMFET biosensor, Nanotechnology 29 (23) (2018) 235203.

[38] G. Wadhwa, B. Raj, Label free detection of biomolecules using charge-plasma-based gate underlap dielectric modulated junctionless TFET, J. Electron. Mater. 47 (2018) 4683–4693.

[39] G. Wadhwa, B. Raj, Design, simulation and performance analysis of JLTFET biosensor for high sensitivity, IEEE Trans. Nanotechnol. 18 (2019) 567–574.

[40] S.P. Adhikari, P. Vukelich, D.C. Guenther, S. Karmakar, P.J. Hrdlicka, Recognition of double-stranded DNA using LNA-modified toehold Invader probes, Org. Biomol. Chem. 19 (42) (2021) 9276–9290, https://doi.org/10.1039/D1OB01888D, 10.1039/D1OB01888D.

[41] S. Sahay, M.J. Kumar, Junctionless Field-Effect Transistors: Design, Modeling, and Simulation, John Wiley & Sons, 2019.

[42] J. Bitra and G. Komanapalli, "A Novel dielectric modulated step-channel junction less TFET (DM-SC-JLTFET) for label-free detection of brest cancer cells: design and sensitivity analysis," 2023.

[43] A.M. Ionescu, Nanowire transistors made easy, Nat. Nanotechnol. 5 (2010) 178–179.

[44] H. Yuehui, H. Ru, G. Yuefeng, F. Liangyou, Impact of process variability on threshold voltage in vertically-stacked nanosheet TFET, Silicon (2023) 1–9.

[45] D. Chowdhury, et al., A novel dielectric modulated gate-stack double-gate metal-oxide-semiconductor field-effect transistor-based sensor for detecting biomolecules, Sensors 23 (6) (2023), https://doi.org/10.3390/s23062953.

[46] A. Shadman, E. Rahman, Q.D.M. Khosru, Monolayer MoS2 and WSe2 double gate field effect transistor as super nernst pH sensor and nanobiosensor, Sens. Biosens. Res. 11 (2016) 45–51, https://doi.org/10.1016/j.sbsr.2016.08.005, 2016/12/01/.

[47] N. Chowdhury, G. Iannaccone, G. Fiori, D.A. Antoniadis, T. Palacios, GaN nanowire n-MOSFET with 5 nm channel length for applications in digital electronics, IEEE Electron Device Lett. 38 (7) (2017) 859–862.

[48] B.V. Chandan, K. Nigam, D. Sharma, Junctionless based dielectric modulated electrically doped tunnel FET based biosensor for label-free detection, Micro Nano. Lett. 13 (4) (2018) 452–456, https://doi.org/10.1049/mnl.2017.0580.

[49] J. Li, et al., Enzyme-based multi-component optical nanoprobes for sequence-specific detection of DNA hybridization, Adv. Mater. 20 (3) (2008) 497–500.